

# Oxygen-Dependent Auto-Oscillations of Water Luminescence Triggered by the 1264 nm Radiation

Sergey V. Gudkov,<sup>†,‡</sup> Vadim I. Bruskov,<sup>\*,†,‡</sup> Maksim E. Astashev,<sup>‡,§</sup> Anatoly V. Chernikov,<sup>†</sup> Lev S. Yaguzhinsky,<sup>||</sup> and Stanislav D. Zakharov<sup>⊥</sup>

<sup>†</sup>Institute of Theoretical and Experimental Biophysics, Russian Academy of Sciences, Pushchino, Moscow Region, 142290 Russia

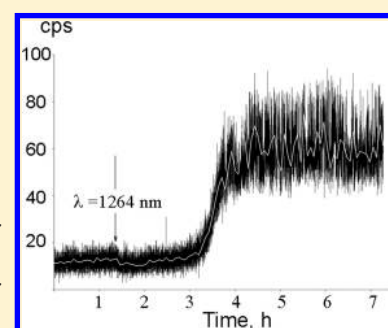
<sup>‡</sup>Pushchino State University, Pushchino, Moscow Region, 142290 Russia

<sup>§</sup>Institute of Cell Biophysics, Russian Academy of Sciences, Pushchino, Moscow Region, 142290 Russia

<sup>||</sup>Lomonosov Moscow State University, Vorob'evy Gory, Moscow, 119899 Russia

<sup>⊥</sup>Lebedev Physical Institute, Russian Academy of Sciences, Moscow, 119991 Russia

**ABSTRACT:** A 5-min exposure of air-saturated bidistilled water to low-intensity laser infrared radiation at the wavelength of the electronic transition of dissolved oxygen to the singlet state ( ${}^3\Sigma_g^- \rightarrow {}^1\Delta_g$ ) induces, after a long latent period, auto-oscillations of water luminescence in the blue–green region, which last many hours. Laser irradiation causes the accumulation of hydrogen peroxide, which depends on the concentration of dissolved oxygen. The auto-oscillations do not arise if water is irradiated beyond the oxygen absorption band and if the oxygen is removed from water. The wavelet transform analysis of luminescence records indicates that there are two characteristic periods of pulsations of about 300 and 1150 s. The results obtained suggest that auto-oscillations are triggered by photoinduced singlet oxygen  ${}^1\Delta_g$ , and this phenomenon is closely related to formation of hydrogen peroxide.



## INTRODUCTION

The key role of oxygen in maintaining life is determined by the unique electron structure of its molecule, which is a triplet in the ground state ( $X\ {}^3\Sigma_g^-$ ) (electronic spin 1) and a singlet (spin 0) in electron excited states. The lowest of the excited states,  ${}^1\Delta_g$  (energy 0.98 eV), usually called singlet oxygen ( ${}^1O_2$ ),<sup>1,2</sup> is a highly reactive species with a lifetime in water of about 4  $\mu$ s.<sup>3</sup> Conventionally, singlet oxygen is generated by photosensitizers and is used as an active agent in cancer phototherapy.<sup>4</sup> The direct photoexcitation of  ${}^1O_2$  in suspensions of living cells and protein solutions results in various biological effects, from activation to inhibition, depending on the exposure dose.<sup>5–7</sup> The light–oxygen effect also takes place in physicochemical systems, in particular, in photobleaching of dyes acting as singlet oxygen traps in aqueous solutions,<sup>8</sup> and manifests itself as changes in the acetone spectrum.<sup>9</sup> The spectrum of molecular oxygen has several relatively narrow absorption bands in the visual and near-infrared (IR) regions.  ${}^1O_2$  can be generated by excitation at each band, but the strongest excitation is achieved at a maximum near 1264 nm.<sup>10</sup> Light sources such as cw diode lasers are particularly suitable for generating singlet oxygen since their low intensity enables one to eliminate thermal effects.

It has been shown previously that short-term irradiation of water with a He–Ne laser results in persistent auto-oscillations of luminescence after a long latent period.<sup>11</sup> The 632.8 nm wavelength of the laser falls within an  $O_2$  absorption band ( ${}^3\Sigma_g^- + {}^3\Sigma_g^- \rightarrow {}^1\Delta_g + {}^1\Delta_g$ , 0–0 transition);<sup>8</sup> therefore, we assumed that the phenomenon is initiated by singlet oxygen.

Here, we present experimental evidence in favor of this hypothesis. The transition of dissolved oxygen to the singlet state in water samples exposed to 1264 nm radiation was used because the energy of the photons at this wavelength, unlike the energy of He–Ne photons, is insufficient for excitation of possible organic contaminants.<sup>8,9</sup> As in the case of a He–Ne laser,<sup>11</sup> exposure of water to 1264 nm radiation resulted in luminescence oscillations, which occurred after a long latent period. The luminescence takes place in the blue–green region of the visible spectrum. A mathematical analysis of hidden periodicities of the process revealed 300 and 1150 s rhythms, the last of which agrees well with the previously found oscillation period (18 min) of the ratio of ortho to para nuclear spin isomers and redox potential in pure water.<sup>12</sup>

## EXPERIMENTAL METHODS

**Irradiation.** A sample of bidistilled water (10 mL; electrical conductivity 120  $\mu$ S/m, pH 5.6) in a 20-mL polypropylene vial for liquid scintillation counting (Beckman, United States) was irradiated in the dark at room temperature with a 5 mW diode laser through the open surface by a quartz light guide. The distance from the light guide end to the water surface was about 10 mm, and the mean density of the light flux on the water surface

**Received:** March 11, 2011

**Revised:** April 29, 2011

**Published:** May 19, 2011

was 1 mW/cm<sup>2</sup>. A laser beam cross section was visualized using an IRDC-AS-22 card. In several experiments, the laser was replaced by a 50 mW IR light diode, which emits in the region of 960–985 nm with a maximum at 975 nm.

**Measurement of Luminescence.** A vial with an irradiated sample was placed in a high-sensitivity chemiluminometer Biotoks-7AM (Ekon, Russia) operating in the regime of a photon counter with a sensitivity band at 380–710 nm.<sup>11</sup> The time of signal accumulation and the periodicity of recording the data was 1 s. The efficiency of photon counting was about 10%, as determined by calibration against Cherenkov radiation from isotope <sup>32</sup>P. The region of the luminescence spectrum was estimated using blue or red optical filters with 99% transmission of light flow at 380–520 and 590–800 nm, respectively.

**Measurement of Hydrogen Peroxide.** The concentration of hydrogen peroxide was determined by the method of enhanced chemiluminescence in a system luminol–4-iodophenol–peroxidase.<sup>13</sup> Chemiluminescence intensity was measured using a Beta-1 liquid scintillation counter (Medapparatyura, Russia) in the photon-counting operation mode; calibration was carried out using hydrogen peroxide samples of known concentration.

**Removal of Oxygen from Water.** The concentration of dissolved oxygen was measured on an Ekspert-001 device (Ekoniks, Russia) using a DKTP 02.4 oxymetric electrode. The initial oxygen concentration was about 270 μM. Degassing was carried out by different methods. After evacuation of water followed by freezing and thawing, the oxygen content decreased to 160 μM. The saturation of water with argon by bubbling for 20 min as described in ref 16 led to a decrease in oxygen concentration to 130 μM. Upon heating water to boiling temperature followed by cooling, the oxygen concentration decreased to 50 μM. Because the degassing by heating was most effective, this method was further used.

**Wavelet Transform.** The wavelet transform of the time series of luminescence values makes it possible to reveal the amplitude–frequency and phase–frequency characteristics of signals locally with time. The result of the wavelet transform represents the decomposition of the time series in the basis of soliton-like functions by changes of the scale and transfers.<sup>14</sup> The Morlet basis of the complex wavelet transform of the form<sup>15</sup>

$$\psi(r) = e^{ik_0 r} e^{-r^2/2}$$

was used, where  $k_0$  is the coefficient of angular selectivity of the wavelet. We took  $k_0 = 2\pi$ ; thus, with  $r = 1$ , the harmonic component of the wavelet has a unit wavelength. The scale translations were carried out by the equation

$$\psi_j(a) = |a|^{-1/2} \psi\left(\frac{j}{a}\right)$$

where  $a$  is the scale coefficient equal to the wavelength of the harmonic component of the wavelet and  $j$  is the number of the element. With allowance for the discrete character of the time series and limitation of the integration range, the equation for calculation of wavelet coefficients takes the form

$$W(a, b) = \sum_{j=-L/2}^{L/2} X_{j+b} \psi_j(a)$$

where  $b$  is the parameter of temporal shift,  $X_j$  is the  $j$ th element of the initial monomeric signal,  $L$  is the length of the filter, which was determined from the relation  $L = 5a$ . Transforming a

monomeric signal by the complex basis function yields dimeric arrays of values of the module and phase of coefficients of the form

$$W(a, b) = |W(a, b)| e^{i\Phi(a, b)}$$

Further, the module of the wavelet transform coefficients was analyzed.

**Method of Detrended Fluctuation Analysis.** A search for latent correlations in the series was performed by the method of detrended fluctuation analysis (DFA)<sup>16</sup> with a modification.<sup>17</sup> In this method, the fluctuation function  $F_2(l)$  is related to the time window  $l$  (length of splitting) by an equation

$$F_2(l) \approx l^H$$

where  $H$  is the Hurst exponent, which is determined from the slope of function  $F_2(l)$  built in double-logarithmic coordinates. The reliability of the conclusions obtained by DFA and the wavelet transform was controlled by randomly mixing the initial series of data. The procedure of mixing consists of the following steps

- 1 Choosing the experimentally obtained time series of values  $\{X_i\}$ , where  $i = 1 \div N$  and  $N$  is the length of the series.
- 2 Two integer random numbers ( $a$  and  $b$ ) in the range  $1 \div N$  were generated.
- 3 The values of the series  $X_a$  and  $X_b$  were interchanged.
- 4 Steps 2 and 3 were repeated  $1000 \times N$  times, which provided a complete mixing of the initial series.

## RESULTS

**Description of the Phenomenon.** The effect induced by 1264 nm laser irradiation of an aqueous sample did not manifest itself within 1.5–2.5 h after exposure: the intensity of luminescence of the sample did not exceed the background level ( $10 \pm 5$  counts per second, cps). Then the luminescence began to increase and reached  $42 \pm 3$  cps ( $n = 16$ ) over a period of 20–40 min with the subsequent transition to the auto-oscillation mode (Figure 1, insets 1 and 2). The process continued for 16–22 h. Exposure of the same sample to laser radiation after cessation of auto-oscillations did not lead to their repeated trigger. Thus, after irradiation of water at 1264 nm, three successive stages of the process were observed: (1) a latent period, (2) origination and increase of luminescence, and (3) quasiperiodic auto-oscillations. The exposure of water samples to 975 nm radiation resulted neither in a distinct luminescence increase nor in auto-oscillations despite a 10-fold increase in treatment intensity. The luminescence of control samples not exposed to laser radiation did not substantially change over a period of six and more hours ( $n = 10$ ) and remained at the background level. A typical record for control samples is given in Figure 1 to the right of the arrow.

**Analysis of Time Series by DFA.** The data obtained in experiments with the laser (1264 nm) after the increase in the luminescence (both the entire record and its separate parts) were analyzed by the DFA method. In addition, the randomly mixed data of all variants of the experiment were considered. The results of the analysis of the region with quasiperiodic changes in luminescence (time interval from 4 to 7 h in Figure 1) are shown in Figure 2. The Hurst exponent  $H = 0.82$  indicates a persistent dynamics of changes in water luminescence. The time series corresponding to the region of the quasiperiodic mode contained from 8973 to 21 614

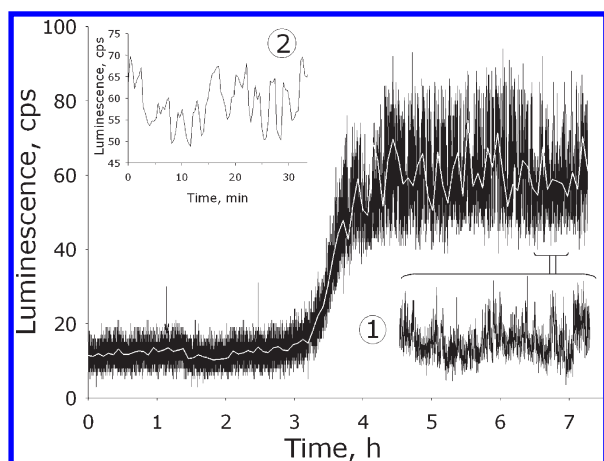


**Figure 1.** Effect of laser radiation on water luminescence. The data of a representative experiment are shown. Water was exposed to an infrared laser ( $\lambda = 1264$  nm, power 5 mW) for 5 min. The time of exposure is shown by a vertical arrow. To the left of the arrow is a record of the background water luminescence before the onset of laser irradiation. The white line on the basic plot presents the macrostructure of a signal obtained using the smoothing option of the program SigmaPlot. Inset 1 shows the microstructure of changes in water luminescence. In inset 2, the integral intensity of water luminescence corresponding to that in inset 1 is given.

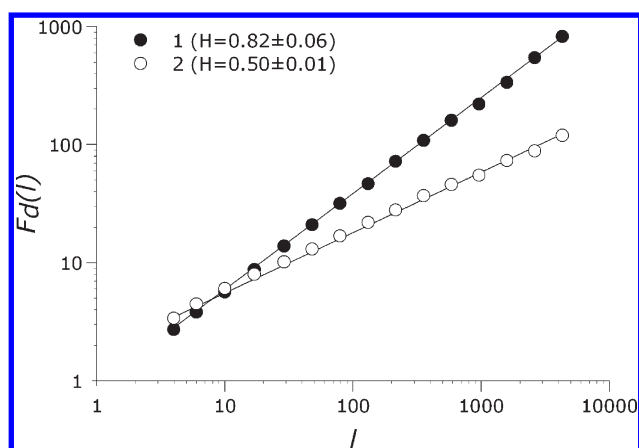


**Figure 2.** Dependence of the fluctuation function  $F_d$  on the time window length  $l$  on double-logarithmic scale as determined by DFA: (1) for a time series in experiments with laser; (2) for the same samples of time series mixed in a random manner.

events in each of 16 experiments with 1264 nm laser radiation. The  $H$  value was  $0.82 \pm 0.06$  (the standard error is given). For control records ( $n = 10$ ),  $H$  was  $0.51 \pm 0.01$ ; this value is characteristic for a random process. The Hurst exponent for water luminescence after treatment with a light diode at 975 nm was also close to the value typical of a random process. To confirm that the high value of the Hurst exponent is related to a regular sequence of fluctuations rather than the distribution of signal amplitudes, the standard test of random mixing of signals was performed. It was found that the Hurst exponent for randomly mixed time series is equal to  $0.50 \pm 0.01$ , confirming the reliability of the analysis. The scatter of values for mixed sequences (2%) indicates the accuracy of the DFA method.

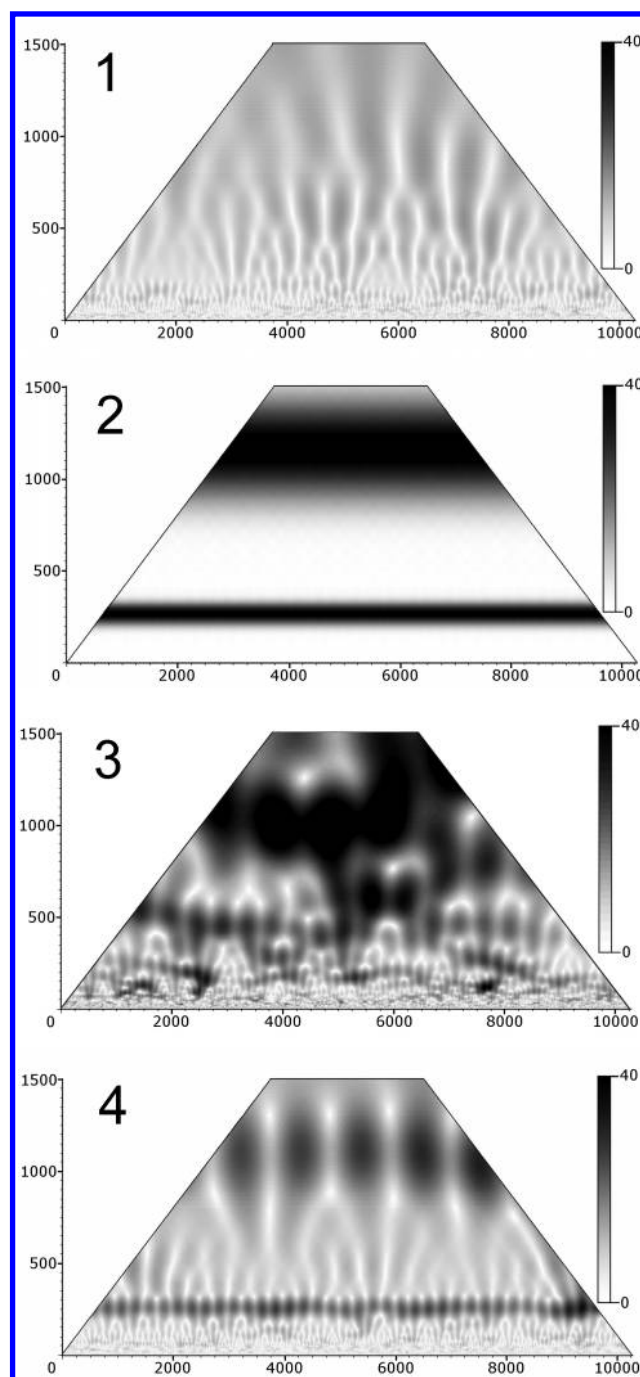


**Figure 3.** Maps of wavelet coefficients that reveal harmonics in the time series. The ordinate axis corresponds to the scale coefficient, which characterizes the wavelengths identified during the analysis, and the abscissa axis corresponds to the parameter of a shift, which determines the temporal localization of the harmonic. The gray scale characterizes the value of the modulus of the wavelet coefficient: (1) a random signal (mixed data and the data of control experiments); (2) a model signal ( $y = \sin(2\pi x/l_1) + \sin(2\pi x/l_2)$ , where  $l_1 = 250$ ;  $l_2 = 1250$ ); (3, 4) patterns typical for luminescence at the stage of auto-oscillations.

**Analysis of Time Series by the Wavelet Transform.** The method of complex wavelet transform is most adequate for detecting the particular frequencies in time series. The adequacy of applying the wavelet analysis was verified by using a model



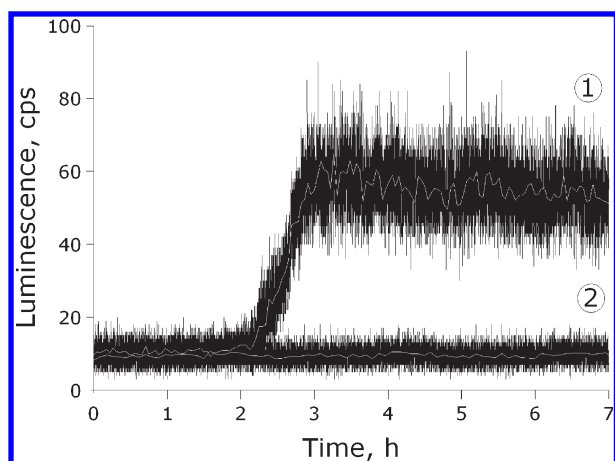


**Figure 4.** Estimation of the spectral region of water luminescence. The intensity of luminescence, as estimated using light filters: (1) blue light filter; (2) red light filter. The smoothed signal is obtained using the smoothing option of the SigmaPlot software package (white line).

signal containing two harmonics with frequencies that differed more than two times. Figure 3 (2) shows a wavelet map for the function  $y = \sin(2\pi x/l_1) + \sin(2\pi x/l_2)$ , where  $l_1 = 250$ ;  $l_2 = 1250$ , i.e., the two frequencies differ five times. Two solid stable lines are seen on the wavelet map. By analyzing the mixed data (including the model signal) and the data of control experiments, it is impossible to detect the isolated frequencies, which confirms the reliability of subsequent treatment of the data (Figure 3, 1). In 7 out of 16 experiments with the 1264 nm laser (44%), persistent auto-oscillations were observed throughout the registration period (Figure 3, 4). In 3 out of these 7 cases, harmonics with periods of about 300 and 1150 s were observed simultaneously, whereas in the remaining cases one of these harmonics dominated. In 9 experiments (56%), a nonstationary oscillatory mode was registered; in this case, in about 50% of the cases, only one of these periods was clearly defined. In addition, the period of the oscillatory mode tended to change. Thus, the period of one oscillatory mode of about 1150 s somewhat increased during the experiment, whereas the other period (about 500 s at the beginning of the experiment) decreased to 300 s (Figure 3, 3).

**Dependence of the Effect on the Oxygen Content in Water.** Two approaches were used to verify whether the triggering of auto-oscillations is related to excitation of oxygen dissolved in water. The oxygen concentration in samples was lowered to about 50  $\mu\text{M}$  (see the Experimental Methods) compared with the equilibrium value of 270  $\mu\text{M}$ . After exposure of such degassed water to 1264 nm radiation, the luminescence intensity remains at the level of background values over a period of 6 h and more. After saturation of degassed water with atmospheric air, irradiation with the laser led again to three characteristic phases of luminescence shown in Figure 1.

**Estimation of the Spectral Region of Water Luminescence.** The region of the spectrum of water luminescence induced by the IR laser was estimated using blue and red optical light filters. With the use of the red optical filter, luminescence phases 2 and 3 were absent and the luminescence corresponded to the background level. With a blue light filter, the situation was similar to that observed in the absence of the filter (Figure 4), i.e., the luminescence occurred in the blue–green region of the visible spectrum.

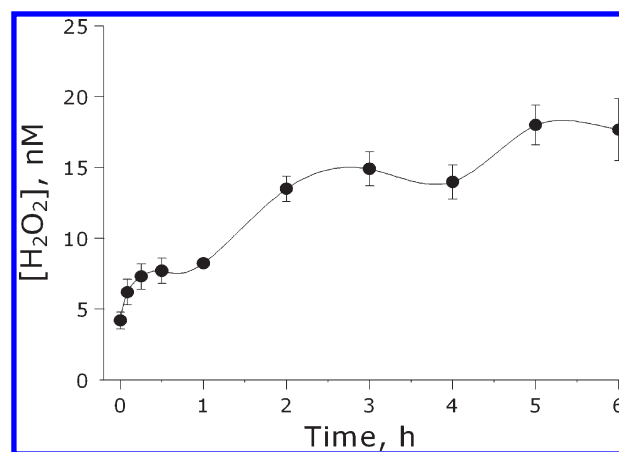


**Figure 5.** Kinetics of hydrogen peroxide formation after a 5-min exposure of a water sample to laser radiation at 1264 nm.

**Generation of Hydrogen Peroxide.** In a sample exposed to 1264 nm radiation, formation of hydrogen peroxide occurs (Figure 5). The concentration of  $\text{H}_2\text{O}_2$  at 5 min after laser treatment increases by 2 nM. Within an hour, the concentration of hydrogen peroxide increases insignificantly to about 8 nM. Then, the average concentration of hydrogen peroxide increases to about 15 nM over a period from 1 to 3 h and to about 18 nM over a period from 5 to 6 h.

We examined whether the concentration of dissolved oxygen, the presence of scavengers of singlet oxygen, and addition of  $\text{D}_2\text{O}$  affect the photoinduced generation of  $\text{H}_2\text{O}_2$ . The data obtained are presented in Table 1. In a water sample with a 2.6-fold higher oxygen content, the concentration of  $\text{H}_2\text{O}_2$  after irradiation with an IR laser increased 2.7 times (Table 1). On saturation of water with argon, when the oxygen concentration in water decreased approximately 2-fold, the rate of  $\text{H}_2\text{O}_2$  generation decreased, correspondingly, two times. Addition of 25%  $\text{D}_2\text{O}$ , which increases the lifetime of singlet oxygen, led to an increase in the  $\text{H}_2\text{O}_2$  generation, as it occurred by the action of heat.<sup>18,19</sup> Sodium azide, a scavenger of singlet oxygen, and tiron (4,5-dihydroxy-1,3-benzenedisulfonate), a scavenger of superoxide radicals,<sup>18,19</sup> partially prevented the  $\text{H}_2\text{O}_2$  generation by laser radiation (Table 1). Sodium azide inhibited  $\text{H}_2\text{O}_2$  generation by 60% (Table 1). The effect of tiron and superoxide dismutase (SOD) on the light-induced generation of  $\text{H}_2\text{O}_2$  in water indicates the involvement of superoxide anion radicals in this process. Tiron at a concentration of 100 nM induced a 2-fold decrease in the content of hydrogen peroxide (Table 1). Addition of SOD led to a more than 2-fold increase in  $\text{H}_2\text{O}_2$  formation, due to dismutation of superoxide radicals by the action of this enzyme (Table 1).

## DISCUSSION

Earlier it was reported that purified water luminesces in the UV and blue–green regions of the spectrum under ionizing radiation<sup>20</sup> and UV light,<sup>21–23</sup> but if the source of radiation is switched off, luminescence terminates. The distinguishing feature of the luminescence observed in the present work is that it arises after a prolonged period of time following irradiation and has an auto-oscillatory mode. Besides, it is initiated by infrared photons whose energy (0.98 eV) is insufficient for ionization of water molecules or generation of free radicals. The energy dose of

**Table 1. Effect of Various Compounds on Hydrogen Peroxide Formation in Bidistilled Water Exposed to Laser Radiation (1264 nm) for 5 min**

test sample	change in hydrogen peroxide concentration,	
	nM <sup>a</sup>	k <sup>b</sup>
H <sub>2</sub> O, equilibrated with air (control)	2.0 ± 0.2	1
H <sub>2</sub> O, saturated with Ar <sup>c</sup>	0.2 ± 0.1 <sup>d</sup>	0.1
H <sub>2</sub> O, saturated with O <sub>2</sub> <sup>c</sup>	5.4 ± 0.7 <sup>d</sup>	2.7
D <sub>2</sub> O, 25% (v/v)	4.2 ± 0.8 <sup>d</sup>	2.1
sodium azide, 0.1 mM <sup>e</sup>	0.8 ± 0.2 <sup>d</sup>	0.4
SOD, 10 <sup>-3</sup> U/mL	4.4 ± 0.8 <sup>d</sup>	2.2
tiron, 100 nM	1.0 ± 0.4 <sup>d</sup>	0.5

<sup>a</sup> The initial values of the hydrogen peroxide concentration in water were subtracted from the values obtained after exposure. The data are the means ± standard error of means of at least three separate experiments.

<sup>b</sup> k, relative change in H<sub>2</sub>O<sub>2</sub> concentration by the action of the agent examined. <sup>c</sup> Water was saturated for 15 min by bubbling with gas prior to the laser treatment. <sup>d</sup> Significantly different from control (*P* < 0.05, Student's unpaired *t* test). <sup>e</sup> Sodium azide at this concentration did not markedly inhibit the activity of peroxidase.

0.15 J/mL released within 5 min is too small to produce a marked thermal influence. The absorption coefficient of water at 1260 nm is  $\sim 1 \text{ cm}^{-1}$ ; <sup>24</sup> therefore, incident radiation (1.5 J) is almost completely absorbed in aqueous samples. The absorbed energy is mainly transformed to rotovibrational excitations of H<sub>2</sub>O molecules, which results in an insignificant (by less than 0.03 K) heating of the sample. <sup>25</sup> Only a small part of energy ( $\sim 10^{-6}$  J) is absorbed by dissolved oxygen molecules to transform them into the singlet state as it is estimated in ref 10. The total energy radiated by photons of the sample in the blue–green region during the auto-oscillation ( $\sim 20$  h) with allowance for the quantum yield of the photodetector and the spatial angle of recording was estimated to be  $\sim 10^{-9}$  J.

The 975-nm radiation, which lies beyond the oxygen absorption bands, induces no auto-oscillations, although the energy released in the sample is two times higher than the energy adsorbed at 1264 nm. If the dissolved oxygen concentration decreases from 270 to 50  $\mu\text{M}$ , auto-oscillations do not arise in a sample exposed to 1264 nm radiation. However, after the equilibrium with atmosphere is established again, the repeat irradiation of the sample at 1264 nm results in renewal of auto-oscillations. This indicates that the process is triggered by the photoinduced generation of singlet oxygen. Moreover, it is probable that the photoinduced generation of singlet oxygen leads to the accumulation of some portion of adsorbed energy in water in the form of a particular long-lived state. The superslow relaxation to the original state is accompanied by the release of this additional energy and manifests itself partially in the physicochemical processes observed.

The data obtained indicate that the generation and accumulation of hydrogen peroxide play an important role in this process. It can be assumed that in water a successive reduction of oxygen is initiated: oxygen—singlet oxygen—superoxide (hydroperoxide radical)—hydrogen peroxide, similar to what happens by the action of heat. <sup>18,19,26,27</sup> The luminescence of water in the blue–green region may also be due to recombination of radicals arising from cavitation of nanoscale air bubbles <sup>28</sup> during their collapse as

in the case of sonoluminescence. <sup>29,30</sup> It is likely that this process may be initiated by the transition from the triplet to the singlet state. The results of this study allow one to consider water as an active excitable medium. Water sonoluminescence is characterized by a broad spectrum in the region of 300–500 nm. <sup>31,32</sup> During sonoluminescence, a water molecule is decomposed into the radicals of atomic hydrogen and hydroxyl:  $\text{H}_2\text{O} \rightarrow \text{H}^\bullet + \text{OH}^\bullet$ , which then recombine to form hydrogen peroxide and hydrogen molecules. Other explanations are not ruled out. Therefore, further studies are needed to elucidate the nature of luminescence auto-oscillations.

The phenomenon of auto-oscillations in pure water is of interest in terms of their possible effect on the kinetics of biochemical reactions. The wavelet analysis revealed two characteristic frequencies during the auto-oscillations of water luminescence, which differ 2–4 times. Pulsations with a “long” period of about 1150 s are most steady. This period of oscillations agrees well with a period of oscillations (about 18 min) in the relative content of ortho and para nuclear spin isomers in vapors over the surface of pure water and oscillations in the redox potential of water. <sup>12</sup> It is noteworthy that Chernikov observed oscillations of the light scattering in water and aqueous protein solutions with periods in the regions of 1–6 and 15–20 min, which is close to the values recorded in this work. <sup>33</sup>

## CONCLUSIONS

Auto-oscillatory phenomena such as the Belousov–Zhabotinsky reaction and oscillations of the concentrations of intermediate products in the system of biochemical reactions during glycolysis have been known for a long time. The results presented above show that a similar phenomenon is triggered in pure water by direct photogeneration of singlet oxygen. Measurement of intrinsic luminescence reveals some details of the temporal response of water. Following a long-term delay, the radiation intensity rises above the background level and undergoes many-hour quasiperiodic oscillations. The hydrogen peroxide concentration begins to increase already at the latent stage, suggesting a chain or avalanche character of physicochemical reactions occurring in water. An immediate cause of the oscillating luminescence is likely the recombination of free radicals.

Dissolved oxygen is a photon target providing the start of a chain process leading to the generation of H<sub>2</sub>O<sub>2</sub>. However, this is not its single role. Oxygen can be a participant of radical reactions. The energy generated during the reduction of O<sub>2</sub> to H<sub>2</sub>O<sub>2</sub> can be used for the maintenance of auto-oscillations. The wavelet analysis of time series obtained in luminescence measurements discovers two characteristic rhythms of about 300 and 1150 s, the latter of which is close to the rhythm of fluctuations of the redox potential and the ortho to para ratio of nuclear spin isomers of water found earlier. <sup>12</sup> Though the mechanism of the phenomenon is not clear, its possible linkage to the degree of freedom of water spin represents a promising direction in water dynamics studies. The results obtained also indicate that molecular oxygen present in cells and biological fluids may be one of photoacceptors during the action of laser radiation on biological objects in the region of absorption of molecular oxygen. Formation of H<sub>2</sub>O<sub>2</sub>, which fulfils the signaling and regulatory roles in biological processes, may serve as a mechanism of the therapeutic effect of this laser radiation. <sup>34,35</sup>

## AUTHOR INFORMATION

## Corresponding Author

\*Phone: +7 4967 739497. Fax: +7 4967 330553. E-mail: bruskov\_vi@rambler.ru.

## ACKNOWLEDGMENT

This work was conducted at the Institute of Theoretical and Experimental Biophysics, Russian Academy of Sciences. We thank Ms. Svetlana V. Sidorova for her assistance in preparing the manuscript. This work was supported by the Russian Foundation for Basic Research (projects nos. 10-04-00800-a, 10-04-00949-a, 10-02-90301-Viet-a) and a grant of the President of the Russian Federation for the support of young scientists (project MK-108.2010.4).

## REFERENCES

- (1) Foote, C. S.; Clennan, E. L. In *Active Oxygen in Chemistry*; Foote, C. S., Valentine, J. S., Greenberg, A., Liebman, J. F., Eds.; Chapman and Hall: London, 1995; pp 105–140.
- (2) Schweitzer, C.; Schmidt, R. *Chem. Rev.* **2003**, *103*, 1685–1758.
- (3) Skovsen, E.; Snyder, J. W.; Lambert, J. D. C.; Ogilby, P. R. *J. Phys. Chem. B* **2005**, *109*, 8570–8573.
- (4) Henderson, B. W.; Dougherty, T. J. *Photochem. Photobiol.* **1992**, *55*, 145–157.
- (5) Zakharov, S. D.; Ereemeev, B. V.; Perov, S. N. *Sov. Phys.-Lebedev Inst. Rep.* **1989**, *1*, 19–22.
- (6) Zakharov, S. D.; Ivanov, A. V.; Wolf, E. B.; Danilov, V. P.; Murina, T. M.; Nguen, K. T.; Novikov, E. G.; Panasenko, N. A.; Perov, S. N.; Skopinov, S. A.; Timofeev, Yu. P. *Quantum Electron.* **2003**, *33*, 149–162.
- (7) Zakharov, S. D.; Ivanov, A. V. *Biophysics* **2005**, *50* (Suppl. 1), 64–85.
- (8) Krasnovsky, A. A., Jr.; Drozdova, N. N.; Ivanov, A. V.; Ambartsumian, R. V. *Biochemistry (Moscow)* **2003**, *68*, 963–966.
- (9) Anquez, F.; Courtade, E.; Sivery, A.; Suret, P.; Randoux, S. *Opt. Express* **2010**, *18*, 22928–22936.
- (10) Zakharov, S. D.; Ivanov, A. V. *Quantum Electron.* **1999**, *29*, 1031–1053.
- (11) Bruskov, V. I.; Gudkov, S. V.; Chalkin, S. F.; Smirnova, E. G.; Yaguzhinskii, L. S. *Dokl. Biochem. Biophys.* **2009**, *425*, 114–116.
- (12) Morre, D. J.; Orczyk, J.; Hignite, H.; Kim, C. J. *Inorg. Biochem.* **2008**, *102*, 260–267.
- (13) Gudkov, S. V.; Shtarkman, I. N.; Smirnova, V. S.; Chernikov, A. V.; Bruskov, V. I. *Radiat. Res.* **2006**, *165*, 538–545.
- (14) Astafeva, N. M. *Phys. Usp.* **1996**, *39*, 1085–1108.
- (15) Grossmann, A.; Morlet, J. *SIAM J. Math. Anal.* **1984**, *15*, 723–736.
- (16) Peng, C.-K.; Buldyrev, S. V.; Havlin, S.; Simons, M.; Stanley, H. E.; Golberger, A. L. *Phys. Rev. E* **1994**, *49*, 1685–1689.
- (17) Kantelhardt, J. W.; Zschiegner, S. A.; Koscielny-Brude, E.; Bande, A.; Halvin, S.; Stanley, E. *Physica A* **2002**, *316*, 87–114.
- (18) Bruskov, V. I.; Masalimov, Zh. K.; Chernikov, A. V. *Dokl. Biochem. Biophys.* **2002**, *384*, 181–184.
- (19) Bruskov, V. I.; Malakhova, L. V.; Masalimov, Zh. K.; Chernikov, A. V. *Nucleic Acids Res.* **2002**, *30*, 1354–1363.
- (20) Quickenden, T. I.; Que Hee, S. S. *Radiat. Res.* **1971**, *46*, 28–35.
- (21) Lobyshev, V. I.; Shikhinskaya, R. E.; Ryzhikov, B. D. *J. Mol. Liq.* **1999**, *82*, 73–81.
- (22) Belovolova, L. V.; Glushkov, M. V.; Vinogradov, E. A.; Babintsev, V. A.; Golovanov, V. I. *Phys. Wave Phenom.* **2009**, *17*, 21–31.
- (23) Chai, B.; Zheng, J.; Zhao, Q.; Pollack, G. H. *J. Phys. Chem. A* **2008**, *112*, 2242–2247.
- (24) Hale, G. M.; Querry, M. R. *Appl. Opt.* **1973**, *12*, 555–563.
- (25) Zakharov, S. D.; Thanh, N. C. *J. Russ. Laser Res.* **2008**, *29*, 558–563.
- (26) Bruskov, V. I.; Chernikov, A. V.; Gudkov, S. V.; Masalimov, Zh. K. *Biophysics* **2003**, *48*, 942–949.
- (27) Smirnova, V. S.; Gudkov, S. V.; Chernikov, A. V.; Bruskov, V. I. *Biophysics* **2005**, *50*, 236–242.
- (28) Bunkin, N. F.; Suyazov, N. V.; Shkirin, A. V.; Ignatiev, P. S.; Indukaev, K. V. *J. Chem. Phys.* **2009**, *130*, 134308–134312.
- (29) Razumovsky, S. D. *Oxygen-Basic Species and Properties*; Khimia: Moscow, 1979.
- (30) Margulis, M. A. *Phys. Usp.* **2000**, *170*, 263–287.
- (31) Didenko, Yu. T.; Pugach, S. P.; Kvochka, V. I.; Nastich, D. N. *J. Appl. Spectrosc.* **1992**, *56*, 618–622.
- (32) Hatanaka, S.; Mitome, H.; Yasui, K.; Hayashi, S. *J. Am. Chem. Soc.* **2002**, *124*, 10250–10251.
- (33) Chernikov, F. R. *Biofizika* **1986**, *31*, 596–600[in Russian].
- (34) Stone, J. R.; Yang, S. *Antioxid. Redox Signal* **2006**, *8*, 243–270.
- (35) Forman, H. J.; Maiorino, M.; Ursini, F. *Biochemistry* **2010**, *49*, 835–842.